A FINITE ELEMENT METHOD FOR SIMULATING INTERFACE MOTION

H.H. YU and Z. SUO
Department of Mechanical and Aerospace Engineering, Princeton Materials Institute
Princeton University, Princeton, NJ 08544

ABSTRACT

This paper describes our recent progress in developing a finite element method for simulating interface motion. Attention is focused on two mass transport mechanisms: interface migration and surface diffusion. A classical theory states that, for interface migration, the local normal velocity of an interface is proportional to the free energy reduction associated with a unit volume of atoms detach from one side of the interface and attach to the other side. We express this theory into a weak statement, in which the normal velocity and any arbitrary virtual motion of the interface relate to the free energy change associated with the virtual motion. An example with two degrees of freedom shows how the weak statement works. For a general case, we divide the interface into many elements, and use the positions of the nodes as the generalized coordinates. The variations of the free energy associated with the variations of the nodal positions define the generalized forces. The weak statement connects the velocity components at all the nodes to the generalized forces. A symmetric, positive-definite matrix appears, which we call the viscosity matrix. A set of nonlinear ordinary differential equations evolve the nodal positions. We then treat combined surface diffusion and evaporation-condensation in a similar method with generalized coordinates including both nodal positions and mass fluxes. Three numerical examples are included. The first example shows the capability of the method in dealing with anisotropic surface energy. The second example is pore-grain boundary separation in the final stage of ceramic sintering. The third example relates to the process of mass reflow in VLSI fabrication.

INTRODUCTION

When a solid is held at an elevated temperature for some time, its structure changes. A film may break into droplets, and an interconnect may grow cavities. The changes are brought about by atomic movements such as diffusion, and motivated by the reduction of free energy such as surface energy. For a bulk material, a detailed knowledge of its microstructure is less critical because an overall knowledge, such as the grain size distribution and pore volume fraction, is often adequate. For a film or a line, where the grain size is comparable to the film thickness and line width, an overall knowledge of structure is inadequate; for example, in submicron aluminum interconnects, the electromigration damage relates to structural details, e.g., crystalline texture and individual grain-boundary orientation [1]. The feature size in integrated electronic circuits is now close to 100 nanometers. For such a small structure, the details of the structure and their evolution are essential to its performance. We can now analyze deformation in complex structures using finite element computer codes. Can we develop a similar tool for evolving structures? This paper describes the recent development of an approach that treats surface motion in a way that resembles the finite element analysis of deformation. The approach naturally combines multiple mass transport mechanisms and energetic forces. For clarity we will introduce the method for interface migration first and then for combined surface diffusion and evaporation-condensation. Surface diffusion alone can be treated as a liming case by setting a very small evaporation-condensation rate.

Mat. Res. Soc. Symp. Proc. Vol. 529 © 1998 Materials Research Society

INTERFACE MIGRATION

Weak Statement

Our method is built upon a weak statement of the interface migration problem. Here we outline its main features; more detailed discussion are given in [2]. Consider an interface separating either two phases of the same atomic composition, or two grains of the same crystalline structure. The interface migrates when the material on one side grows at the expense of the material on the other side. The motion is driven by the reduction of total free energy associated with the motion. Let γ be the surface energy density, which may depend on crystalline orientation. Let g be the difference in the free energy density of the two phases. In evaporation-condensation it is the free energy increase associated with the condensation of unit volume of solid. The total free energy is

$$G = \gamma A + gV , \tag{1}$$

where A is the area of the interface and V the volume of the solid phase. If γ is anisotropic, the total surface energy is a sum over all the facets, or an integral over the entire interface. Thermodynamics requires that the reaction proceed to decrease the free energy.

Define a quantity p such that

$$\int p \delta r_n dA = -\delta G , \tag{2}$$

where δr_n is the virtual motion of the interface, and δG the free energy change associated with the virtual motion. The virtual motion is a small movement in the direction normal to the interface that need not obey any kinetic law. It is an arbitrary function of the position of the interface. Consequently, equation (2) defines the quantity p at every point on the interface. It has the unit of pressure and is the free energy reduction per unit interface area moving per unit distance.

The interface migrates as atoms leave one side and attach to the other side. The actual normal velocity of the interface is a function of the driving pressure. We adopt the linear kinetic relation:

$$v_n = mp . \tag{3}$$

Here m is the mobility of the interface, which is a given quantity in the simulation.

Eliminating p from (2) and (3), we have

$$\int \frac{v_n}{m} \delta r_n dA = -\delta G . \tag{4}$$

Equation (4) holds for any distribution of the virtual motion, δr_n. We refer to (4) as the *weak statement* of the interface migration problem. It has a weaker requirement on the smoothness of the interface than that of the conventional method described by a set of partial differential equations. When the surface tension γ is isotropic, the weak statement is equivalent to the curvature driven migration. When γ is anisotropic, the curvature driven migration is incorrect,

but the weak statement remains valid. The following example shows how this weak statement works.

An Example

Figure 1 shows a crystal having anisotropic surface tension such that it grows into a prism with a square cross-section. When a small particle of such a crystal is introduced into its vapor, it has two degrees of freedom: both the base side B and the height C can change. We need to determine the side and height as functions of time, $B(t)$ and $C(t)$. The surface tension on the prism bases and sides are γ_1 and γ_2, and the mobilities are m_1 and m_2. When the crystal grows by a unit volume at the expense of the vapor, the phase change alone increases the free energy by g. In this discussion, we assume that g is a constant independent of B and C. The total free energy of the system, relative to the vapor without the particle, is

$$G(B,C) = 2\gamma_1 B^2 + 4\gamma_2 BC + gB^2 C. \tag{5}$$

Associated with the virtual changes δB and δC, the free energy varies by

$$\delta G = (4\gamma_1 B + 4\gamma_2 C + 2gBC)\delta B + (4\gamma_2 B + gB^2)\delta C. \tag{6}$$

The kinetic term on the left-hand side of (4) is

$$\int \frac{v_n}{m}\delta r_n dA = \frac{\dot{B}BC}{m_2}\delta B + \frac{\dot{C}B^2}{2m_1}\delta C. \tag{7}$$

The superimposed dot stands for a time derivative. The weak statement (4) requires that both the coefficients before δB and δC vanish, giving

$$\dot{B} = -m_2\left(\frac{4\gamma_1}{C} + \frac{4\gamma_2}{B} + 2g\right) \qquad \dot{C} = -m_1\left(\frac{8\gamma_2}{B} + 2g\right) \tag{8}$$

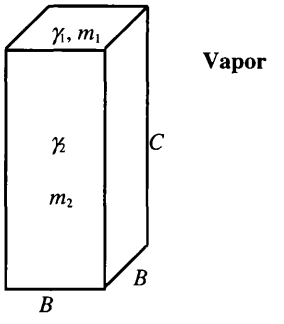

Figure 1. A crystal having anisotropic surface tension grows in its vapor to a prism with a square cross-section.

These are coupled nonlinear ordinary differential equations for the two functions $B(t)$ and $C(t)$, which can be integrated numerically once the initial particle dimensions are given.

Finite Element Method

Equation (4) can be solved numerically by finite element method. We have developed a finite element program for simulating evaporation-condensation [3]. The general procedure is similar to the one we just illustrated in the above example. We approximate an interface by many small elements. The interface is then represented by the positions of all the nodes which are the generalized coordinates $q_1, q_2, q_3, \ldots, q_{3n-2}, q_{3n-1}, q_{3n}$, where n is the total number of the nodes. The generalized velocities are $\dot{q}_1, \dot{q}_2, \dot{q}_3, \ldots, \dot{q}_{3n-2}, \dot{q}_{3n-1}, \dot{q}_{3n}$ and the virtual motion of the interface is represented by $\delta q_1, \delta q_2, \delta q_3, \ldots, \delta q_{3n-2}, \delta q_{3n-1}, \delta q_{3n}$. The velocity and virtual motion of a point on the interface can be interpolated by the values of the nodes. Do the integration in the weak statement (4) element by element, we get a bilinear form in $\dot{q}$ and δq similar to (7). The right-hand side of (4) is the total free energy change associated with the virtual motion,

$$\delta G = -\sum f_i \delta q_i , \tag{9}$$

which allows us to compute the generalized forces $f_1, f_2, \ldots, f_{3n}$. Collect the coefficient of δq_i, giving

$$\sum_j H_{ij} \dot{q}_j = f_i . \tag{10}$$

Equation (10) is a set of linear algebraic equations for the velocity components. Once solved, they update the nodal positions for a small time step. The process is repeated for many steps to evolve the interface. Because the matrix $\boldsymbol{H}$ and force column $\boldsymbol{f}$ depend on the coordinates of all the nodes $\boldsymbol{q}$, (10) is a nonlinear dynamical system. $\boldsymbol{H}$ is a symmetric and positive-definite matrix, which we call the viscosity matrix.

Numerical Example

Figure 2 shows a numerical example of a grain growing in a vapor. The surface energy is anisotropic with a four-fold symmetry,

$$\gamma(\theta) = \gamma_0 \left(1 + |\theta|\right) \qquad \text{for } |\theta| \le \pi/4 .$$

Figure 3 is the polar plot of the surface energy density. The dash-dot line represents the corresponding Wulff shape. In Fig. 2, we start with a small particle with the surfaces having high surface energy density. The particle is immersed in the vapor which has a higher phase energy density than the particle. The normalized phase energy density difference between the particle and the vapor is $ga_0/\gamma_0 = 3.0$, with a_0 being the half diagonal length of the initial particle. The particle grows and, at the same time, forms small facets with the lowest surface energy density. These small facets finally disappear and the final shape of the particle is the same as the Wulff shape in Fig. 3. The size of the small facets in the simulation is not physical; it depends on the size of the finite elements. The trend in the simulation should be correct.

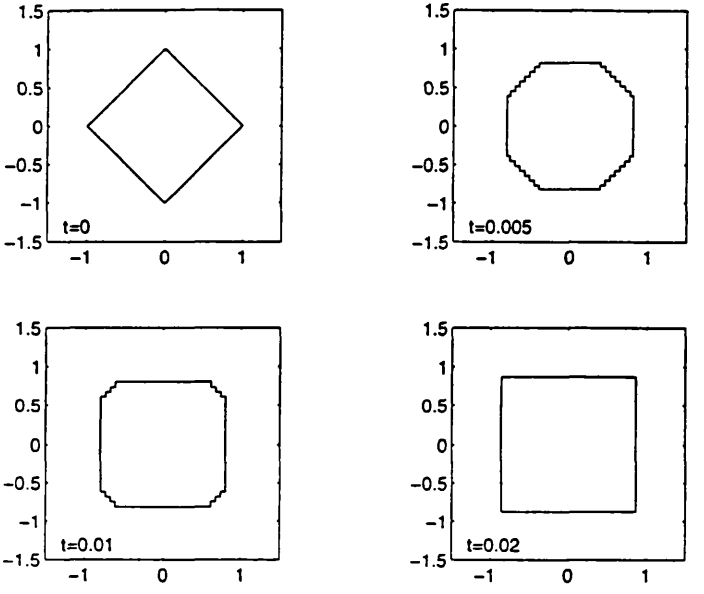

Figure 2. Anisotropic crystal growth in a vapor. The surface energy depends on surface orientation and has a four-fold symmetry. The particle evolves to the Wulff shape.

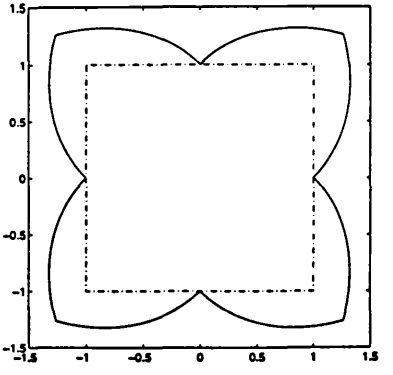

Figure 3. Polar plot of the surface energy density of the particle. The Wulff shape is a square.

The simulation should have captured the general feature of anisotropic grain growth. The unit of time in Fig. 2 is $a_0^2/m\gamma_0$, with m being the mobility of the surface.

SURFACE DIFFUSION AND EVAPORATION-CONDENSATION

Weak Statement

Sun and Suo [4] formulated the weak statement for combined surface diffusion and evaporation-condensation. Imagine two concomitant processes on a surface: the solid matter can relocate on the surface by diffusion, and exchange with the surrounding vapor by evaporation-condensation. The combination of these two processes reduces the total free energy of the system. The relocation of the atoms on the surface and the mass exchange between solid and vapor both change the geometry of the surface. For a polycrystalline particle, its surface intersects with some grain boundaries. The geometric change of the surface will also change the total grain boundary area. So the total free energy change should include the change due to energy density difference between solid and vapor, the change of interfacial energy due to area, and the change of the orientation of the surface and grain boundaries.

Figure 4 illustrates a surface in three dimensions. Denote the unit vector normal to the surface element by $\boldsymbol{n}$. An arbitrary contour lies on the surface, with the curve element dl, and the unit vector $\boldsymbol{m}$ in the surface and normal to the curve element. At a point on the contour, $\boldsymbol{m}$ and $\boldsymbol{n}$ are perpendicular to each other, and both are perpendicular to the tangent vector of the curve at the point. Mass flux $\boldsymbol{J}$ is a vector field tangent to the surface and is defined such that $\boldsymbol{J}\cdot\boldsymbol{m}$ is the volume of atoms crossing unit length of the curve in unit time. The mass exchange between the solid and vapor is represented by flux j, the volume of matter added to a unit area of the solid surface per unit time due to evaporation-condensation. Both the mass flux $\boldsymbol{J}$ due to surface diffusion and the mass flux j from the vapor to the solid change the geometry of the surface. Mass conservation relates the surface velocity, v_n, to the fluxes of the two matter transport processes:

$$v_n = j - \nabla\cdot\boldsymbol{J}. \tag{11}$$

If we neglect the surface diffusion part in (11), j is the normal velocity of the surface. This is the case we considered in the last section for interface migration alone.

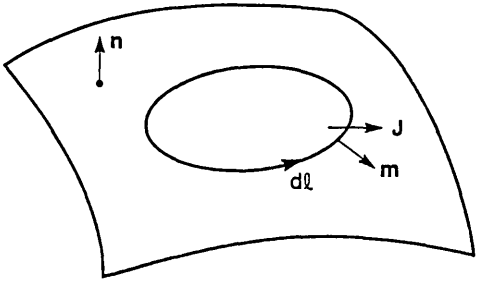

Figure 4. A surface in three dimensions.

The virtual motion due to surface diffusion can be represented by a vector field $\delta \boldsymbol{I}$ tangent to the surface, defined such that $\delta \boldsymbol{I} \cdot \boldsymbol{m}$ is the volume of atoms crossing a unit length of the curve. The virtual motion due to evaporation-condensation can be expressed by δi, the volume of matter added to a unit area of the solid. The two kinds of virtual mass fluxes give the surface a virtual normal displacement,

$$\delta r_n = \delta i - \nabla \cdot (\delta \boldsymbol{I}). \tag{12}$$

Associated with the virtual motion, the free energy changes by δG. Define both the driving pressure p for evaporation-condensation and the driving force $\boldsymbol{F}$ for surface diffusion in one integral form,

$$\int (\boldsymbol{F} \cdot \delta \boldsymbol{I} + p \delta i) dA = -\delta G. \tag{13}$$

The integral extends over all the surface areas participating in mass transfer. The equation holds for any virtual motion. Because $\delta \boldsymbol{I}$ is arbitrary, the local quantity $\boldsymbol{F}$ is prescribed by this global statement. This definition is equivalent to Herring's [5] definition in which the driving force for surface diffusion, $\boldsymbol{F}$, is the amount of free energy decrease associated with per unit volume of matter moving per unit distance on the surface. $\boldsymbol{F}$ is also a vector field tangent to the surface. When the surface tension is isotropic, the definition in (13) can reproduce the relation between the driving force and the curvature gradient [5]. The weak statement is valid for anisotropic surface tension. The weak statement also enforces the local equilibrium condition at the triple junction where three interfaces meet.

Following Herring, we write a kinetic law that, at every point on the surface, the flux is proportional to the driving force:

$$\boldsymbol{J} = \boldsymbol{M}\boldsymbol{F}. \tag{14}$$

Here $\boldsymbol{M}$ is the mobility of atoms for surface diffusion. We assume that the mobility is isotropic. It is represented by a number M, related to the self-diffusivity by the Einstein relation, $M = \Omega D \delta / kT$, where Ω is the volume per atom, D the self-diffusivity on the surface, δ the effective thickness of atoms participating in matter transport, k Boltzmann's constant, and T the absolute temperature.

The kinetic law for evaporation-condensation is the same as (3),

$$j = mp, \tag{15}$$

where m is the specific rate of evaporation-condensation.

Substituting (14) and (15) into (13), we obtain that

$$\int \left(\frac{\boldsymbol{J} \delta \boldsymbol{I}}{M} + \frac{j \delta i}{m} \right) dA = -\delta G. \tag{16}$$

This is the *weak statement* for the combined evaporation-condensation and surface diffusion.

In formulating a finite element method, it is convenient to use $\delta \boldsymbol{I}$ and δr_n as the basic variables. Eliminating j and δi in (16) by using (11) and (12), we obtain that

$$\int \left\{ \frac{\boldsymbol{J} \cdot \delta \boldsymbol{I}}{M} + \frac{(v_n + \nabla \cdot \boldsymbol{J})[\delta r_n + \nabla \cdot (\delta \boldsymbol{I})]}{m} \right\} dA = -\delta G. \tag{17}$$

In this form, the weak statement only involves two virtual fields, δr_n and $\delta \boldsymbol{I}$. They vary independently, subject to no constraint. The free energy change on the right-hand side of (17) includes the energy change associated with the phase transformation and the interfacial energy change associated with the area and orientation change of the surface and grain boundaries.

Surface diffusion alone can be treated as a limiting case. In this situation, matter only diffuses on the surface but does not exchange between the solid and the vapor. Thus we set a small value to m in (17). In this case, the free energy change on the right-hand side of (17) associated with the phase transformation can be neglected. Only the surface energy and grain boundary energy need be considered. If λ is a representative length in a problem, the dimensionless parameter $m\lambda^2 / M$, measures the relative rate of evaporation-condensation and surface diffusion. In the numerical simulation, we set $m\lambda^2 / M = 10^{-6}$.

Finite Element Implementation

Same as the method for interface migration, we can solve $\boldsymbol{J}$ and v_n in (17) numerically by finite element method [4]. We can divide the surface into many small elements, and interpolate $\boldsymbol{J}$ and v_n on each element by their values at the nodes of the element. The generalized coordinates include both the positions and the fluxes of the nodes. Evaluate both the left-hand side and the right-hand side of (17) and collect the coefficients of the virtual motion coordinates,

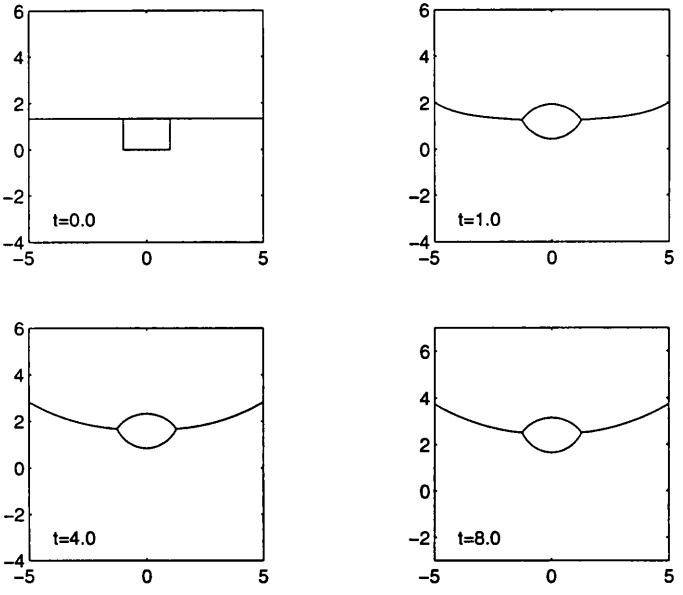

(a)

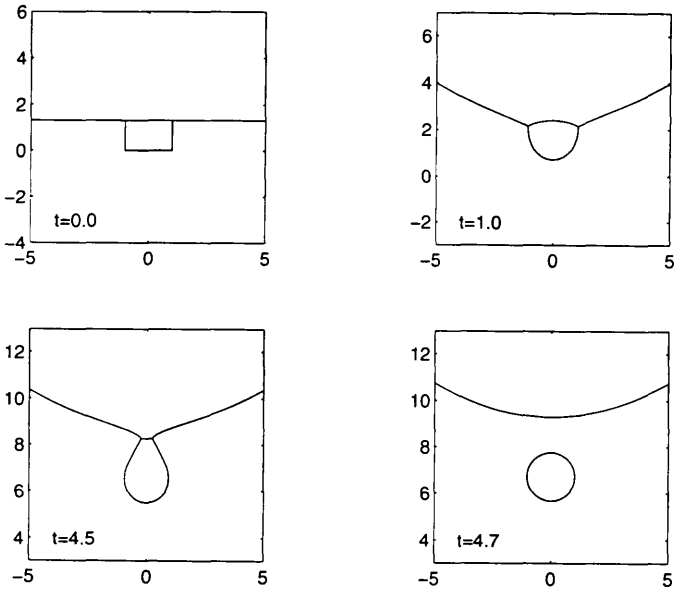

(b)

Figure 5. Pore-grain boundary interaction. A grain boundary is dragged by a force f_b exerted at the outside edge of the simulating unit. The grain boundary migrates. The pore accommodates its position by surface diffusion. In both simulations, we choose $\gamma_B/\gamma_S = 1.0$, $f_b/\gamma_S = 0.5$ and $R/r_0 = 5.0$. a) Pore-grain boundary attachment, $mr_0^2/M = 1.0$; b) Pore-grain boundary separation, $mr_0^2/M = 10$.

and we obtain a set of linear algebraic equations for the velocity and flux components of all the nodes. Solving the equations, we can update the nodal positions for a small time step. The process is repeated for many steps to evolve the surface.

Pore-Grain Boundary Separation

Yu and Suo [6] developed a finite element program for simulating three dimensional axisymmetrical microstructure evolution. The program was used to simulate the process of pore-grain boundary separation. In the final stage of ceramic sintering, the individual pores are isolated on grain boundaries. At this stage, some grains may grow by grain boundary motion. A pore on a migrating grain boundary may either migrate with, or break away from, the grain boundary. The pore accommodates its position by evaporation-condensation, surface diffusion, and volume diffusion. For a small pore, surface diffusion dominates [7,8]. In our simulation, we just considered the surface diffusion of the pore and the grain boundary migration. We

focused on the process of separation, and neglected the grain boundary diffusion in our simulation.

Figure 5 shows two examples. In our simulation, we prescribed a force f_b at the outside edge (a circle) of the simulation unit. This force may represent the force exerted by other grain boundaries intersecting with the migrating grain boundary. The dimensionless parameters are the ratio of grain boundary energy and surface energy γ_B/γ_S ; the normalized prescribed force f_b/γ_S ; the relative rate of grain boundary migration and surface diffusion mr_0^2/M , with m being the mobility of the grain boundary, M the mobility of the surface diffusion and r_0 the radius of a sphere which has the same volume as the pore; the ratio of the radius of the simulation unit and the pore size R/r_0 . R can be considered as the grain size. In our simulation, we took the initial pore shape to be a cylinder. In Fig. 5a, the pore changes the initial shape and finally moves with grain boundary at a constant velocity. The angles at the triple junction quickly evolve to the equilibrium dihedral angles. This local equilibrium condition is enforced by the weak statement naturally. In Fig. 5b, with all other parameters held the same as in Fig. 5a, we changed the relative mobility, mr_0^2/M . In this case the surface diffusion of the pore is so slow compared with the grain boundary migration that the pore cannot accommodate its position quickly enough to catch up with the movement of the grain boundary. Finally the pore separates from the grain boundary. Once trapped inside the grain, the pore heals into a sphere. The unit of time is $r_0^4/M\gamma_S$, and all the lengths are normalized by r_0.

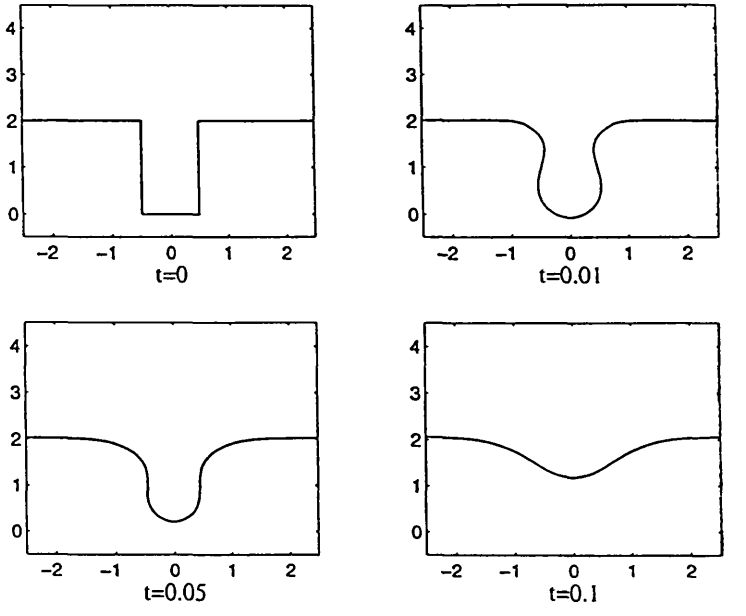

(a)

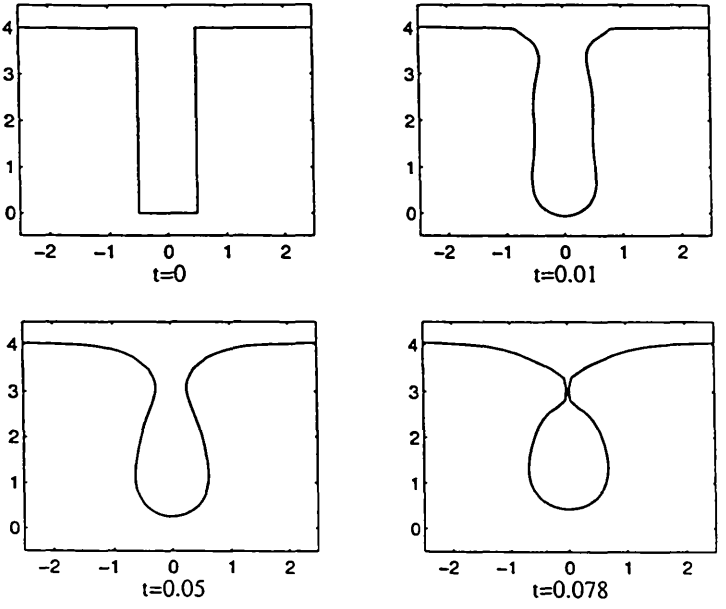

(b)

Figure 6. Mass reflow in a cylindrical hole. a) Mass fills the hole with aspect ratio $d/h = 1/2$; b) A void forms in the hole with aspect ratio $d/h = 1/4$.

Mass Reflow

Mass reflow on a free surface with deep trenches and vias is used in fabricating metal interconnects. After a metal thin film is deposited on a substrate at a low temperature, the trenches and vias on the substrate are not fully filled with the metal. The metal film is then heated to some temperature so that mass can diffuse on the surface. Mass on the platforms can flow into the trenches and vias, which result in the desired interconnects. However, sometimes voids may form before mass fills in the trenches and vias [9]. Gardner and Fraser [10] simulated the effect of trench dimension and film thickness on the mass flow. Huang, Gilmer and de la Rubia [11] developed an atomistic simulator for thin film deposition in three dimensions and simulated the mass reflow of Al thin film. Sun [12] simulated the mass reflow both in a trench and a hole by using the finite element method described in this paper. Figure 6 is the simulation for mass reflow in an axisymmetric hole. In Fig. 6a, the aspect ratio of the hole diameter over the hole depth is $d/h = 1/2$. The hole can be filled without the formation of void. In Fig. 6b, the aspect ratio of the hole diameter over the hole depth is $1/4$, the void is formed before the hole is filled completely. In Fig. 6, the unit time is $d^4/M\gamma_s$. All the lengths are normalized by *d*.

SUMMARY

We have described the finite element method for simulating interface motion due to interface migration and surface diffusion. The method is based on a weak statement which has a weaker requirement on the smoothness of simulating surface than that of the conventional motion by curvature method. The method can handle surface energy anisotropy. The triple junction at which three interfaces meet automatically evolves to the equilibrium dihedral angles. Numerical examples demonstrate that the method can capture the intricate details in transient motions. The method can readily include multiple energetic forces and rate processes, and is applicable to diverse problems with large geometry change.

ACKNOWLEDGEMENTS

The work is supported by the National Science Foundation through a Young Investigator Award and by the Institute for Materials Research and Engineering, Singapore.

REFERENCES

1. C.V. Thompson and J.R. Lloyd, MRS Bulletin, December 1993, p. 19 (1993).
2. Z. Suo, Advances in Applied Mechanics **33**, p.194 (1997)
3. B. Sun, Z. Suo and W. Yang, Acta Mater. **45**, p.1907 (1997).
4. B. Sun and Z. Suo, Acta Mater. **45**, p. 4953 (1997).
5. C. Herring, in The Physics of Powder Metallurgy, edited by W.E. Kingston, pp. 143-179, McGraw-Hill, New York (1951).
6. H.H. Yu and Z. Suo, unpublished work.
7. P.G. Shewmon, Trans. Met. Soc. AIME **230**, p.1134 (1964).
8. C.H. Hsueh and A.G. Evans, Acta Metall. **31**, p.189 (1983).
9. Y. Arita, N. Awaya, K. Ohno and M. Sato, MRS Bulletin **19**, p.66 (1994).
10. D.S. Gardner and D.B. Fraser, Presentation in MRS conference, spring, 1995.
11. H. Huang, G.H. Gilmer and T. D. de la Rubia, An atomic simulator for thin film deposition in three dimensions, preprint (1997).
12. B. Sun, Ph.D. thesis, University of California at Santa Barbara, p.39 (1996).